ORIGINAL ARTICLE

Flow Cytometric Analysis of Mononuclear Phagocytes in Nondiseased Human Lung and Lung-Draining Lymph Nodes

A. Nicole Desch[1,2,3*], Sophie L. Gibbings[4*], Rajni Goyal[4], Raivo Kolde[2,3], Joe Bednarek[4], Tullia Bruno[1], Jill E. Slansky[1], Jordan Jacobelli[1], Robert Mason[5], Yoko Ito[5], Elise Messier[5], Gwendalyn J. Randolph[6], Miglena Prabagar[4], Shaikh M. Atif[4], Elodie Segura[7,8], Ramnik J. Xavier[2,3], Donna L. Bratton[4], William J. Janssen[5], Peter M. Henson[1,4], and Claudia V. Jakubzick[1,4]

[1]Department of Immunology and Microbiology, University of Colorado Denver Anschutz Campus, Denver, Colorado; [2]Center for Computational and Integrative Biology, Massachusetts General Hospital and Harvard Medical School, Boston, Massachusetts; [3]The Broad Institute of Massachusetts Institute of Technology and Harvard, Cambridge, Massachusetts; [4]Department of Pediatrics, National Jewish Health, Denver, Colorado; [5]Department of Medicine, National Jewish Health and University of Colorado Denver Anschutz Campus, Denver, Colorado; [6]Department of Pathology and Immunology, Washington University Medical School, St. Louis, Missouri; [7]INSERM U932, Paris, France; and [8]Institut Curie, Paris, France

Abstract

Rationale: The pulmonary mononuclear phagocyte system is a critical host defense mechanism composed of macrophages, monocytes, monocyte-derived cells, and dendritic cells. However, our current characterization of these cells is limited because it is derived largely from animal studies and analysis of human mononuclear phagocytes from blood and small tissue resections around tumors.

Objectives: Phenotypic and morphologic characterization of mononuclear phagocytes that potentially access inhaled antigens in human lungs.

Methods: We acquired and analyzed pulmonary mononuclear phagocytes from fully intact nondiseased human lungs (including the major blood vessels and draining lymph nodes) obtained *en bloc* from 72 individual donors. Differential labeling of hematopoietic cells via intrabronchial and intravenous administration of antibodies within the same lobe was used to identify extravascular tissue-resident mononuclear phagocytes and exclude cells within the vascular lumen. Multiparameter flow cytometry was used to identify mononuclear phagocyte populations among cells labeled by each route of antibody delivery.

Measurements and Main Results: We performed a phenotypic analysis of pulmonary mononuclear phagocytes isolated from whole nondiseased human lungs and lung-draining lymph nodes. Five pulmonary mononuclear phagocytes were observed, including macrophages, monocyte-derived cells, and dendritic cells that were phenotypically distinct from cell populations found in blood.

Conclusions: Different mononuclear phagocytes, particularly dendritic cells, were labeled by intravascular and intrabronchial antibody delivery, countering the notion that tissue and blood mononuclear phagocytes are equivalent systems. Phenotypic descriptions of the mononuclear phagocytes in nondiseased lungs provide a precedent for comparative studies in diseased lungs and potential targets for therapeutics.

Keywords: monocytes; dendritic cells; pulmonary; macrophages; mononuclear phagocytes

(Received in original form July 15, 2015; accepted in final form November 2, 2015)

*Equally contributing authors.

Supported by NIAID Training Grants T32 AI007405 (A.N.D.), HL68864 and HL88138 (P.M.H.), and HL109517 (W.J.J.); ACS grants RSG-08-184-01-L1B (J.E.S.), HL34303 and AI110408 (D.L.B.), ANR-10-IDEX-0001-02 PSL, ANR-11-LABX-0043, and CIC IGR-Curie 1428 (E.S.); and Natalie Zucker Award, Colorado Clinical Translational Sciences Institute and Bioscience Discovery Evaluation Grant Program, Diversity Supplement HL81151 and R01 HL115334 (C.V.J.).

Author Contributions: Prepared manuscript: C.V.J., A.N.D., W.J.J., P.M.H., and G.J.R. Performed experiments: A.N.D., S.L.G., R.G., and C.V.J. Provided tumor lungs: T.B. and J.E.S. Provided expertise in time-lapse video microscopy: J.J. Provided the human lung tissue and cells for sorting: R.M., W.J.J., Y.I., and E.M. Performed the transcriptome analysis: A.N.D., R.K., and R.J.X. All authors provided intellectual input and critical feedback, discussed results, and designed experiments.

Correspondence and requests for reprints should be addressed to Claudia V. Jakubzick, Ph.D., Department of Pediatrics and Immunology, National Jewish Health, 1400 Jackson Street, Denver, CO 80206. E-mail: jakubzickc@njhealth.org

This article has an online supplement, which is accessible from this issue's table of contents at www.atsjournals.org

Am J Respir Crit Care Med Vol 193, Iss 6, pp 614–626, Mar 15, 2016

Originally Published in Press as DOI: 10.1164/rccm.201507-1376OC on November 9, 2015
Internet address: www.atsjournals.org

At a Glance Commentary

Scientific Knowledge: Every day, the human lung is ventilated with 9,000 L of air containing billions of particles and microbes. Although most are trapped and cleared via mucociliary mechanisms, a significant amount reaches the conducting airways and alveoli, where mononuclear phagocytes promote their clearance. We describe mononuclear phagocytes found in the lung with potential access to the airspaces.

What this Study Adds to the Field: This study describes a method that distinguishes extravascular tissue-resident mononuclear phagocytes from cells present within the vascular lumen. The key element of this approach, which has never been described in human lungs, was labeling hematopoietic cells with anti-CD45 antibodies administered via intrabronchial and intravenous routes into the same lobe. This technique was vital because it excluded intravascular cells from cytometic analyses of extravascular mononuclear phagocytes.

The human respiratory tract has a branching structure that terminates in millions of alveoli, whose luminal surface covers an approximate area of 50 to 100 m^2. In comparison to other barrier surfaces, such as the skin (2 m^2) and the gut (10 m^2), this surface area is massive, and therefore, comprises the body's largest interface with the ambient environment. Because of normal respiratory function, the average human exchanges 7,000 to 9,000 L of gas each day and inhales billions of particles, allergens, and microbes. Accordingly, the human lung constitutes a major site for the innate and adaptive immune responses. In this context, cells in the mononuclear phagocyte system (MPS), which consists of macrophages, monocytes, monocyte-derived cells, and dendritic cells (DCs), play critical roles. These roles include clearance of inhaled particulates and microbes, maintenance of lung structure and function, and initiation of immune responses. Therefore, it is not surprising that lung mononuclear phagocytes (MPs) have been demonstrated to play both beneficial and pathogenic roles in a variety of pulmonary diseases including, but not limited to, viral, bacterial, and fungal pneumonia, chronic obstructive pulmonary disease (COPD), asthma, adult respiratory distress syndrome, sarcoidosis, hypersensitivity pneumonitis, and the idiopathic interstitial pneumonias. Therefore, understanding the identity, location, and function of MPs in the lung is of paramount importance to further our understanding of human disease. The primary objective of our study was to categorize the MPs in human lungs using surface immune phenotyping and transcriptome analysis, and to identify their location in terms of tissue and vascular compartments.

In recent years, the framework through which the MPS is viewed has undergone extensive revision, and includes new paradigms regarding the ontogeny, activation states, and functional roles played by its members (1, 2). Elegant studies performed in mice have demonstrated that alveolar macrophages arise during embryogenesis and self-renew throughout life with minimal replacement from circulating cells (3–5). At the same time, the lung also contains tissue macrophages with mixed ontogeny and postnatal-derived monocytes that constitutively migrate through the tissues (6–10). Furthermore, different MPs exist within the extravascular and intravascular compartments, each with its own function and phenotype. Whether these relationships hold true in human lungs remains unclear.

Although other studies have demonstrated unique surface marker expression for macrophage subpopulations in lavage and tissue samples, these studies were limited in their ability to fully determine the compartment in which these cells reside (11–17). In addition, the vessels of surgically resected lung tissue cannot be perfused, making it impossible to disregard MPs within the pulmonary vasculature, which is known to contain a substantial proportion of the circulating pool of leukocytes (18–21). In this study, we analyzed fully intact right lungs (including the major blood vessels and draining lymph nodes) obtained *en bloc* from 72 individual donors who died from nonpulmonary causes and whose right lungs were not transplanted (*see* Table E1 in the online supplement). Using intrabronchial (IB) and intravascular instillation of anti-CD45 antibodies to label cells, we identified five unique populations of extravascular MPs. Some of the results of this study have been previously reported in the form of a conference abstract (22).

Methods

Human Lung MP Isolation

We received de-identified human lungs that were not used for organ transplantation from the National Disease Research Interchange (Philadelphia, PA), the International Institute for the Advancement of Medicine (Edison, NJ), and the University of Colorado Donor Alliance (Denver, CO). We selected donors without a history of chronic lung disease and with reasonable lung function, with a $Pa_{O_2}/F_{I_{O_2}}$ ratio of >225, a clinical history and X-ray that did not indicate infection, and limited time on a ventilator (*see* Table E1). We noted the age, sex, smoking history, cause of death, medical history, and time of death. Nonsmokers were defined as never smoked (*see* Table E1). The Committee for the Protection of Human Subjects at National Jewish Health approved this research.

Lungs were removed *en bloc* in the operating room and included the trachea, lymph nodes (LNs), and pulmonary vessels. Pulmonary arteries were perfused in the operating room with cold histidine-tryptophan-ketoglutarate (HTK) solution to preserve endothelial cell function and prevent intravascular clot formation. The lungs were submerged in HTK and immediately shipped on ice. All lungs were processed within 24 hours of removal. The lungs were visually inspected for lesions or masses and were eliminated from the study if grossly abnormal. Paratracheal, subcarinal, and carinal LNs were identified and removed. Bronchoalveolar lavage (BAL) was performed on the right middle lobe or lingula by completely filling the lobe three times with phosphate-buffered saline (PBS) and 5-mM ethylenediaminetetraacetic acid, and then three times with PBS alone. After each instillation, lavage fluid was drained from the lung, collected, and pooled.

Lung tissue and LNs were minced and enzymatically digested with 2.5 mg/ml collagenase D (Roche, New York, NY) and 0.2 mg/ml liberase (Roche) for 30 minutes at 37°C. Tissue digestion was collected and pressed through a 100-μm nylon filter to obtain single-cell suspensions. Cells were

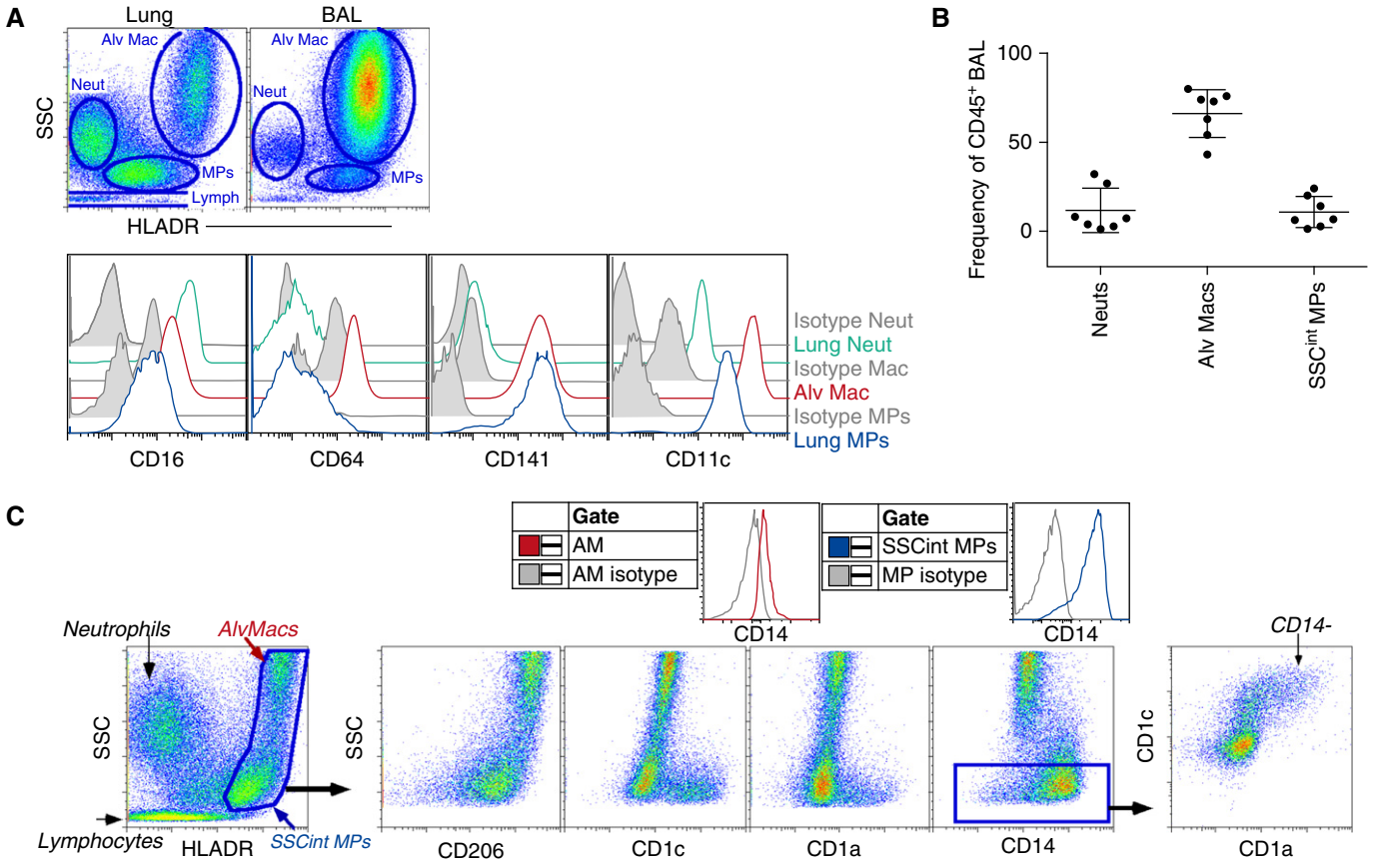

Figure 1. Bulk analysis of lung mononuclear phagocytes (MPs) found in bronchoaveolar lavage (BAL) and cell suspension. (*A*) Alveolar macrophages (Alv Macs), neutrophils (Neuts), and MPs from lung digest and BAL fluid were identified by side scatter (SSC) and human leukocyte antigen (HLA)-DR expression (*top*) and stained for CD64, CD141, and CD11c (*bottom*). Isotype control antibody (*gray*). (*B*) Frequencies of Alv Macs, MPs, and Neuts in BAL fluid. (*C*) HLA-DR$^+$ Alv Macs and intermediate SSC (SSC^{int}) MPs were gated and plotted for the expression of CD206, CD1c, CD1a, and CD14. Isotype controls are shown as *gray* histograms. Flow cytometric data is one representative experiment of at least 10 independent experiments. AM = alveolar macrophages.

re-suspended in fluorescence-activated cell sorter (FACS) blocking solution with pooled human serum 20 min before antibody staining (*see* Table E2) and analysis on the BD LSRII flow cytometer (BD Biosciences, San Jose, CA).

Lung adenocarcinoma samples and tumor adjacent tissues from eight donors were obtained with ethical consent from non-small cell lung carcinoma subject samples through the Lung Cancer Specialized Programs of Research Excellence resource under our National Jewish Health Institutional Review Board–approved protocol.

Intravenous and IB Antibody Delivery

The middle or lower right lobe was used, and the pulmonary artery and lobar bronchus were cannulated. Using 200 μg of PerCP anti-CD45 (clone eBioCB16; eBioscience, San Diego, CA) diluted in 20 ml of PBS, and 500 μg of fluorescein isothiocyanate (FITC) anti-CD45 (clone HI30, BD) diluted in 50 ml of PBS, the antibody was delivered to the pulmonary artery and the lobar bronchus, respectively.

Peripheral Blood Mononuclear Cells Isolation

Blood was obtained by venipuncture from healthy adults as per institutional review board approved protocol. Isolation of peripheral blood mononuclear cells (PBMCs) was by Percoll gradient.

Mixed Leukocyte Reaction

Naive T cells were obtained from healthy donor PBMCs by negative selection using a cocktail of biotinylated anti-CD19, anti-CD20, anti-CD11c, and anti–human leukocyte antigen (HLA)-DR antibodies followed with anti-Biotin magnetic beads (Miltenyi Biotec, San Diego, CA). CD3$^+$ T cells were enriched to >95% purity, labeled with 10-μM carboxyfluorescein succinimidyl ester (CFSE), and plated 30,000 cells per well. Antigen-presenting cells isolated from enzymatically digested lungs were enriched by positive selection using biotinylated anti-CD11c, anti-CD1c, and anti-CD14 antibodies followed by anti-Biotin microbeads. Enriched antigen-presenting cells (stimulators) were co-cultured with T cells (responders) at a 1:1 ratio in Roswell Park Memorial Institute medium with 10% fetal calf serum. At Day 5, T cells were assessed by flow cytometry for CFSE dilution.

Immunofluorescence Analysis on Cryosections

Paratracheal, subcarinal, and carinal LNs were fixed in 4% paraformaldehyde, incubated overnight in 30% sucrose, embedded in tissue-tek OCT (optimal cutting temperature compound) (Sakura), and stored at −80°C. Sections were stained overnight with primary antibodies to CD11c (clone 3.9, eBiosciences), CD14

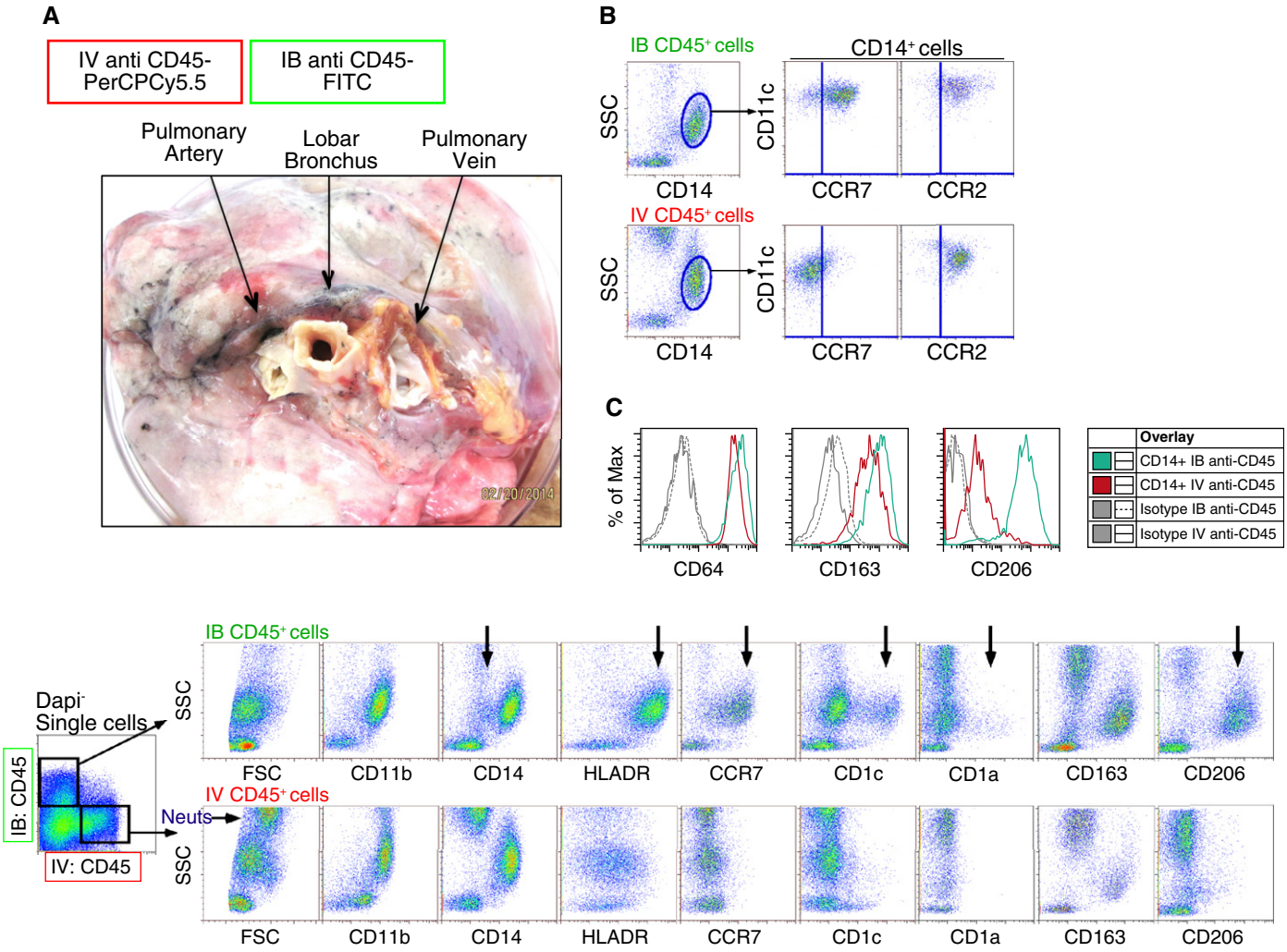

Figure 2. Analysis of human lung mononuclear phagocytes (MPs) following differential labeling via the airspaces and vasculature. (*A*) Differential routes of antibody delivery into human lungs were achieved using the middle right lobe. Anti-CD45 fluorescein isothiocyanate (FITC)-conjugated antibody was delivered into a lobar bronchus (intrabronchial [IB]) and anti-CD45 PerCPCy5.5-conjugated antibody was delivered into the pulmonary artery (intravenous [IV]). The lobar bronchus, pulmonary vein, and pulmonary artery were clamped for 25 minutes before washing and enzymatic digestion. Single-cell suspensions were first gated as live, 4′,6-diamidino-2-phenylindole^{-} (DAPI^{-}) single cells. Then, IB anti-CD45^{+} cells (*upper panel*) and IV anti-CD45^{+} cells (*lower panel*) were plotted as side scatter (SSC) versus various MP markers. Data are representative of at least six different donor lungs. (*B*) Gated CD14^{+}SSC^{int} cells labeled IB (*top*) or IV (*bottom*) were examined for the expression of CCR7 and CCR2. (*C*) Gated CD14^{+} MPs from IB anti-CD45^{+} (*green*) and IV anti-CD45^{+} (*red*) fractions were plotted for the expression of CD64, CD163, and CD206. Isotype controls are *gray*. The *black arrows* (besides the one labeled Neuts) illustrate differences between the MP populations within the extravascular and intravascular spaces. FSC = forward scatter; HLADR = human leukocyte antigen-DR; Neuts = neutrophils.

(Cat. 347,490 BD), CD141 (cat. 130-090-694 Miltenyi Biotec), CD1c (cat. 130-090-695 Miltenyi Biotec), HLA-DR (clone L243, Biolegend, San Diego, CA), or CD20 (clone 2H7, eBioscience), and incubated for 1 hour with fluorochrome-conjugated secondary antibodies or fluorochrome-conjugated streptavidin. Samples were mounted using 4′,6-diamidino-2-phenylindole (DAPI)-containing mounting media (VectaShield, Burlingame, CA) and imaged using a Leica confocal microscope (Leica Microsystems, Buffalo Grove, IL).

Transcriptome Analysis

The 46bp sequences from 3′ ends of the molecules were mapped to the refSeqGene sequences (hg19) using BWA software (Burrows-Wheeler Aligner, Cambridge, UK) (23) with default parameters. Each read was associated with unique molecular identifier (UMI) sequence tagging individual RNA molecules. The expression was quantified as the number of UMIs per gene. The count matrix was further normalized using the variance stabilizing normalization method from DEseq2 (24) in Bioconductor. *P* values and false discovery rate values to determine statistically significant differences between groups were found using the edgeR package (25) in Bioconductor (*see* Table E3).

Results

Identification of Extravascular versus Intravascular Pulmonary MPs

To begin to identify MPs in the lung, we first used cellular granularity (side scatter [SSC])

Table 1. A Summary of Surface Molecule Expression by Extravascular and Blood Mononuclear Phagocytes

	Extravascular Lung					Blood		
	Pulmonary DCs	$CD1a^+$ ModC	$CD1a^-$ ModC	Tissue Monos	Alveolar MACs	$CD141^+$ ($BDCA3^+$) DCs	$CD1c^+$ ($BDCA1^+$) DCs	$CD14^+$ Monos
CD206	−	+	+	+	+	−	−	−
CD14	−	lo	+	+	lo	−	−	+
CD16	−	−	−	+/++	−	−	−	−/+/++
CD11b	−	lo	+	+	+	−	−	+
CD141	−	−	−	+	+	+	−	−
CD1c	+	+	+	−	−	−	+	−
CD1a	+	+	−	−	−	−	−	−
DEC205	−	−	−	−	−	+	−	−
Clec9a	−	−	−	−	−	+	−	−
CD64	−	−	−	+	+	−	−	+

Definition of abbreviations: DCs = dendritic cells; MACs = macrophages; ModC = monocyte-derived cells; Monos = monocytes.

and differential expression of HLA-DR to distinguish different cell populations. Within BAL fluid, alveolar macrophages represented the majority of the leukocytes and displayed distinctively high SSC (Figures 1A and 1B). In contrast, four main leukocyte population clusters were detected in single-cell suspensions of enzymatically digested lung tissue: intermediate-to-high SSC ($SSC^{int/hi}$) $HLA\text{-}DR^-$ granulocytes (predominantly $CD16^+$ neutrophils); $SSC^{hi}HLA\text{-}DR^+$ alveolar macrophages; low SSC (SSC^{low}) $HLA\text{-}DR^{-/+}$ lymphocytes; and $SSC^{int}HLA\text{-}DR^+$ MPs encompassing monocytes and DCs from the blood and lung (Figures 1A and 1B). Evaluation of surface molecules revealed that a portion of $SSC^{int}HLA\text{-}DR^+$ MPs expressed CD206, CD1c, CD1a, and CD14, whereas alveolar macrophages expressed CD64, CD141, and CD206. As recently reported, we also observed that alveolar macrophage expressed low levels of CD14 compared with the $SSC^{int}HLA\text{-}DR^+$ MPs (Figure 1C) (26). Within the $SSC^{int}HLA\text{-}DR^+$ MPs, a $CD1a^+CD1c^+$ population was detected that did not express CD14. Thus, our initial analysis of bulk pulmonary MPs identified alveolar macrophages by high SSC and low CD14 expression, and a mixed population of extravascular and intravascular MPs that differed from macrophages in granularity and surface marker expression previously associated with DCs and monocytes.

To determine whether the detected $SSC^{int}HLA\text{-}DR^+$ MPs were extravascular or intravascular cells, we developed a strategy to identify the leukocytes in the two compartments of the human lung. Before digestion, we co-delivered into a lobe of the right lung (*1*) FITC-conjugated antibody against CD45 through the lobar bronchus (IB), and (*2*) PerCPCy5.5-conjugated CD45 antibody through the main pulmonary artery while clamping the pulmonary vein (intravenously [IV]) (Figure 2A). Clamps were used to close openings to each route, and the lung was gently massaged and stained for 25 min. The lungs were perfused with PBS via the cannulated artery and bronchus to remove excess antibody. Due to the removal of a significant amount of alveolar macrophages upon BAL and filtration after digestion, $SSC^{int}HLA\text{-}DR^+$ MPs represented the majority of MPs within the tissue digest. Therefore, to evaluate surface molecule expression by intravascular and extravascular MPs, a higher SSC setting was used on the cytometer. After digestion, two distinct $CD45^+$ leukocyte populations were detected within the single-cell suspension (Figure 2A). Although both routes of anti-CD45 delivery labeled $SSC^{int}CD14^+CD11b^+$ populations with similar C-C chemokine receptor 2 (CCR2) expression (Figures 2A and 2B), there were significant differences between cells labeled in these two compartments: (1) a $CD14^{low}$ population detected within IB-labeled MPs that was not observed within the IV-labeled MPs (Figure 2A); and (2) among the IB CD45-labeled MPs, there were two unique populations, distinguished by surface expression of $CD1c^+$ and $CD1a^+$, that were not observed among intravascular CD45-labeled MPs (Figure 2A). Lastly, IB CD45-labeled MPs expressed higher levels of HLA-DR, chemokine receptor CCR7, and integrin CD11c, and selectively expressed the mannose receptor, CD206, compared with IV-labeled MPs (Figures 2A–2C). In summary, MPs labeled with antibody delivered to the airspaces were phenotypically disparate from cells labeled in the pulmonary vasculature.

To verify that CD206 expression is restricted to extravascular MPs, we analyzed PBMCs. Peripheral blood $CD14^+$ monocytes and blood DCs (known as $CD1c^+$ and $CD141^+Clec9a^+$ DCs) had no detectable CD206 expression (*see* Figures E1A and E1B). Furthermore, although we observed $CD11c^+CD1a^+$ blood cells, $CD1c^+$ and $CD141^+Clec9a^+$ blood DCs did not stain positively for CD1a (*see* Figure E1A). Therefore, our studies demonstrate that in the nondiseased lung digest, CD206 expression and coexpression of CD1c and CD1a are restricted to extravascular MPs.

Pulmonary MPs Have Distinct Morphology

Next, we illustrated the sorting strategy and morphology of the five pulmonary MPs. Surface expression for pulmonary and blood MPs are summarized in Table 1. First alveolar macrophages were sorted from BAL fluid. The other four pulmonary MPs were enriched using CD11c beads. Enriched cells were first gated on $DAPI^-$ $CD45^+$ Lin^- (CD20, CD3, CD56) cells. Then, these cells were plotted as SSC versus HLA-DR. $SSC^{int}HLA\text{-}DR^{high}$ cells were gated on and sorted using the expression of CD206, CD1c, and CD1a (Figures 3A–3C; for the full gating strategy *see* Figure E2). It was critical to exclude subcellular debris from our gating strategy (*see* Figure E3) because subcellular debris resulted in a false-positive $HLA\text{-}DR^+CD11c^+CD141^+CD11b^-CD14^-$ stain that was $DAPI^-$, and depending on the CD45 fluorochrome used, would appear

CD45 positive. All CD206$^+$ MPs were classified as extravascular pulmonary MPs, whereas CD206$^-$CD1c$^-$ MPs were considered intravascular MPs due to earlier observations that CD206 expression was restricted to IB-labeled, anti-CD45 cells and not circulating PBMCs (Figure 2A; *see* Figure E1B). However, we detected a single extravascular cell population with high CD1c and CD1a expression that displayed no CD206 expression (Figure 3A). This cell was classified as extravascular, because coexpression of CD1c and CD1a was observed exclusively within IB-labeled anti-CD45 cells (Figure 2A) and blood CD1c$^+$ cells did not express CD1a (*see* Figure E1A). As a comparison, one intravascular MP population was examined, CD14$^+$CD206$^-$CD1c$^-$CD1a$^-$ monocytes, which were phenotypically similar to blood CD14$^+$ monocytes and had varying levels of CD16 (Table 1 and Figure 3A).

After sorting, the morphologies of pulmonary MPs were compared with those of blood monocytes and blood DCs. Filopodia are thin, F-actin–dependent protrusions that in macrophages act as tentacles to draw in particles for phagocytosis (27). Blood CD14$^+$ monocytes and all intravascular and extravascular CD14$^+$ pulmonary MPs exhibited long extended filopodia with ruffling, whereas blood B-lymphocytes rapidly clustered together, displaying short filopodia and no ruffling. Alveolar macrophages exhibited large lamellipodial movement (Figure 3C; *see* Videos E1 and E7). Strikingly, CD206$^-$CD1c$^+$CD1a$^+$ lung MPs revealed classical dendrite protrusions with bifurcation and some lamellipodial movement, closely resembling the original description of DCs (Figure 3C; *see* Video E8) (28). Blood CD141$^+$ DCs also displayed classical dendrites with lamellipodia, and blood CD1c$^+$ DCs rapidly moved within the culture system using a lamellapodial leading edge (Figure 3C; *see* Videos E9 and E10 in

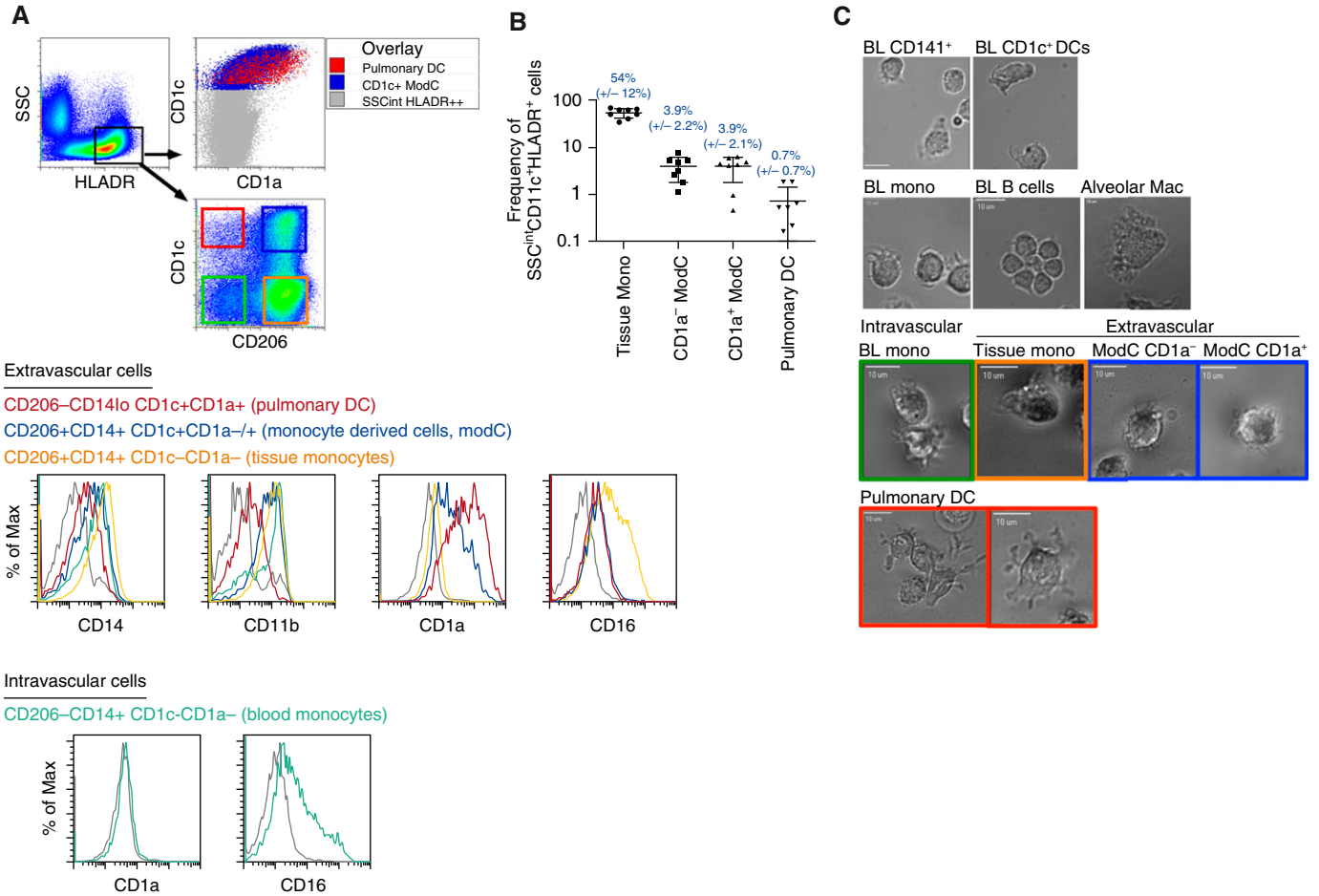

Figure 3. Human lung intermediate side scatter (SSC^{int}) human leukocyte antigen (HLA)-DR$^+$ mononuclear phagocytes (MPs) can be distinguished by the expression of CD206, CD1c, and CD1a. (*A*) CD11c$^+$ cells were enriched from lung digest using macrophage (Mac)-beads and analyzed by flow cytometry. SSC^{int}HLA-DR$^+$ MPs were gated and plotted as CD1c versus CD206 to separate four MP populations. Extravascular CD206$^-$CD1c$^+$ pulmonary dendritic cells (DCs) (*red gate*), CD206$^+$CD1c$^+$ monocyte-derived cells (ModC) (*blue gate*), and CD206$^+$CD1c$^-$ tissue monocytes (Mono) (*orange gate*), and intravascular CD206$^-$CD1c$^-$ monocytes (*green gate*) were stained for surface expression of CD14, CD11b, CD1a, and CD16. Overlay of pulmonary DCs and monocyte-derived cells over all SSC^{int}HLA-DR$^+$ MPs, plotted as CD1c versus CD1a (*top right*). (*B*) Frequencies of extravascular pulmonary MPs found in tissue excluding alveolar Macs. Flow cytometry data is one representative experiment of at least seven independent experiments. (*C*) Video time-lapse image of fluorescence-activated cell-sorted human MPs from peripheral blood (BL) and lung tissue. Data are representative of five separate sorts with 10 to 15 cells per field. *Scale bars* = 10 μm.

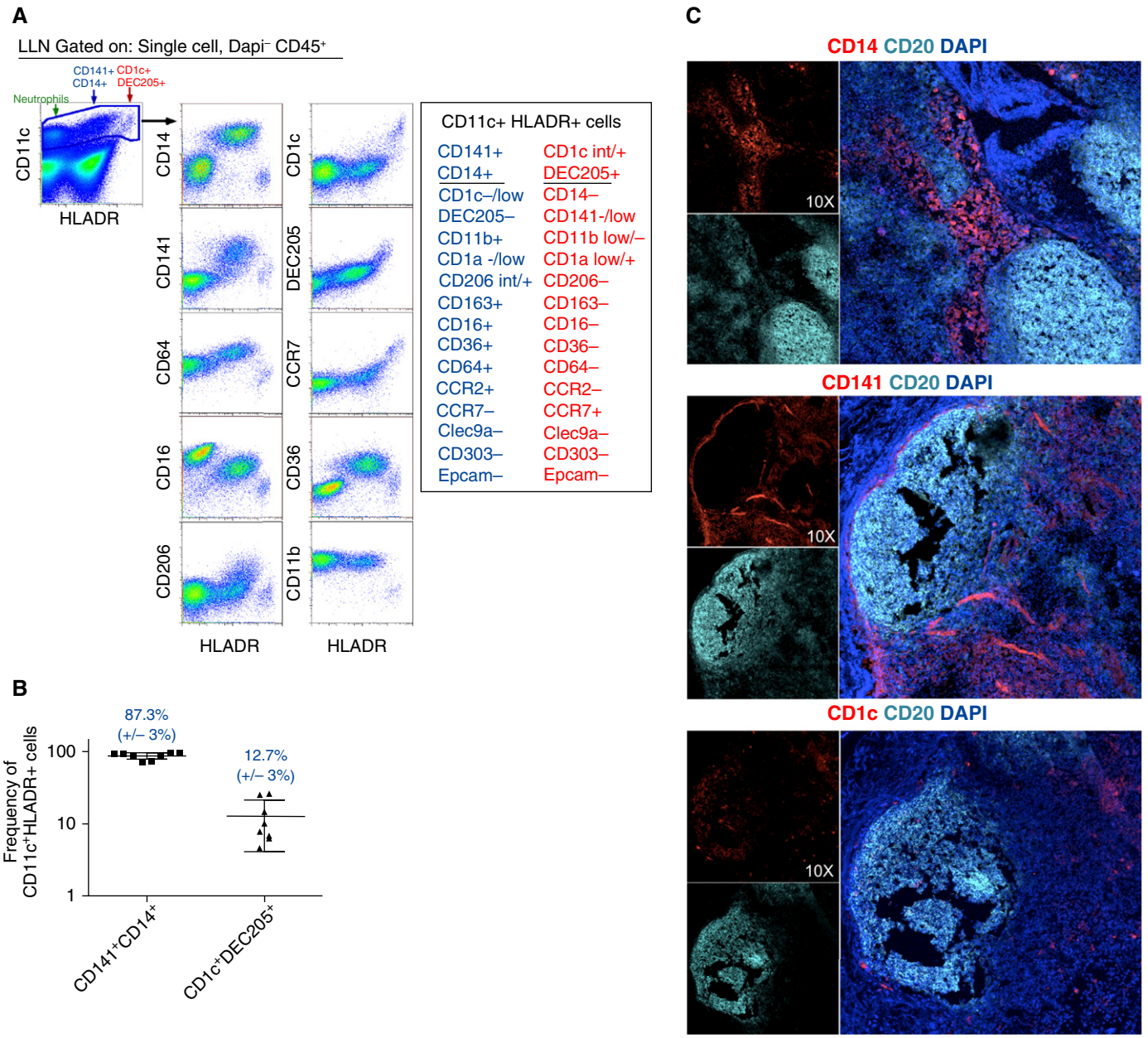

Figure 4. Phenotypic analysis of mononuclear phagocytes (MPs) found in pulmonary lymph nodes. (*A*) $CD11c^+$ human leukocyte antigen (HLA)-DR neutrophils (*green arrow*), HLA-DR^+ $CD141^+CD14^+$ MPs (*blue arrow*), and HLA-DR^{hi} $CD1c^+DEC205^+$ MPs (*red arrows*) isolated from lung-associated lymph nodes (LLNs). Gated $CD11c^+$ cells were then plotted as HLA-DR versus MP markers. (*B*) Frequencies of $CD141^+CD14^+$ MPs and $CD1c^+DEC205^+$ MPs found in LLNs. Each *dot* represents a frequency obtained from individual lungs collected from multiple experiments. (*C*) Three-color immunofluorescence in cryosections of lung-associated LLNs stained for CD20 (*cyan*), 4′,6-diamidino-2-phenylindole (DAPI) (*blue*), and CD14 (*upper, red*), CD141 (*middle*, *red*) or CD1c (*lower*, *red*). Data represent one experiment of eight independent experiments (*A* and *B*) and one experiment of four independent experiments (*C*).

the online supplement). From these analyses, it was determined that of all the five extracellular lung MPs, only $CD206^-CD1c^+CD1a^+$ cells clearly displayed DC morphology (Figure 3C; *see* Videos E3–E8).

In summary, based on surface marker expression and morphological analysis from time-lapse videos, we observed and defined five distinct MPs in the lung. In addition to alveolar macrophages, four other pulmonary MPs were detected. Three $CD14^+CD206^+$ populations displayed monocyte-like morphologies and differential expression of the DC markers CD1c and CD1a: $CD14^+CD206^+CD1c^-CD1a^-$ tissue monocytes (tissue monos); $CD14^+CD206^+CD1c^+CD1a^-$ monocyte-derived cells ($CD1a^-$ ModCs); and $CD14^+CD206^+CD1c^+CD1a^+$ monocyte-derived cells ($CD1a^+$ ModCs). One CD206 negative population displayed DC morphology and expressed low levels of CD14 and CD11b, and high levels of DC markers CD1c and CD1a: $CD14^{lo}CD206^-CD1c^+CD1a^+$ DCs (pulmonary DCs) (Figure 3A and Table 1; *see* Figure E2).

After digestion of the entire right middle lobe, the cellular counts after FACS-sorting yielded (on average) total cell counts of 5.04×10^8 ($\pm 1.57 \times 10^8$), and total alveolar macrophages obtained from BAL were 3.55×10^8 ($\pm 1.95 \times 10^8$). For $CD206^+$ pulmonary MPs, $CD14^+CD1c^-$ 5.7×10^5 ($\pm 5 \times 10^5$), $CD1a^-$ ModC 1.039×10^5 ($\pm 1.059 \times 10^5$), and $CD1a^+$ ModC 8.38×10^4 ($\pm 9.132 \times 10^4$) viable cells were acquired. For the pulmonary DCs, 1.598×10^4 ($\pm 1.817 \times 10^4$) viable cells were acquired.

Identification of MPs and DCs in Lung-associated Lymph Nodes

Migratory DCs link innate and adaptive immune systems by the unique ability to traffic antigens from tissues to draining LNs through expression of the chemokine receptor CCR7 (29–31). Due to the high level of HLA-DR and CCR7 expression in IB-labeled $CD45^+$ cells, we predicted the lung-draining LNs would contain MPs similar to MPs identified in the lung. Digestion of the lung-draining LNs revealed two $CD11c^+$HLA-DR^+ populations that were phenotypically similar to MPs found in the lung: $CD141^+CD14^+$ MPs and $CD1c^+$ MPs (Figures 4A–4C and Table 2). Within LNs, $CD14^+CD141^+$ MPs cells consistently expressed CD206, CD36, CD64, and CD11b with little to no expression of CD1c and CCR7 (Figure 4A and Table 2; *see* Figure E4). Because CCR7-expression is required for migration from tissues to draining LNs, it is unclear whether the $CD141^+CD14^+$ MPs migrated from the lungs or entered the LNs through the high endothelial venules (29–31). In contrast, HLA-DR^{hi} $CD11c^+$ MPs displayed intermediate to high levels of CD1c, high levels of CCR7, and selectively expressed the endocytic receptor DEC-205 and $CD1a^{int/+}$ (Figure 4A and Table 2; *see* Figure E4). LN $CD11c^+$HLA-DR^{hi} $CD1c^+$ MPs displayed multiple phenotypic similarities with pulmonary DCs, including the lack of CD141 expression, no expression of Clec9a, CD14, CD11b, and CD206, and intermediate to high expression of CD1a (Figure 4A; *see* Figure E4). Furthermore, LN $CD1c^+$ cells differed from blood $CD1c^+$ DCs by the high expression of DEC205 and CD1a (Figure 4A, for LN, *see* Figure E4; for blood, *see* Figure E1). Data showing phenotypic similarities and elevated CCR7 expression raise the possibility that LN $CD1c^+$ MPs are lung-derived pulmonary DCs. However, we can only speculate, because these data did not definitively prove that LN $CD1c^+$ MPs were derived from migratory pulmonary DCs.

Within LNs, $CD1c^+$ MPs primarily localized within the T-cell zone with close proximity to the B-cell zone, with sparse $CD1c^+$ cells within the B-cell zone (Figure 4C). In contrast, $CD141^+$ and $CD14^+$ cells were detected exclusively within the T-cell zone (Figure 4C), with some $CD141^{bright}$ cells representing endothelial cells present throughout the subcapsular sinus and B-cell zone. Based on the location of the two identified LN MPs, it is likely that they interact with T cells within lung-draining LNs.

$CD1c^+$ DCs Are Superior T-Cell Stimulators in a Mixed Leukocyte Reaction

A distinctive feature of DCs is the superior ability to stimulate T-cell responses. We tested the T-cell stimulatory capacities of $CD14^+$ and $CD1c^+$ MPs isolated from the lung in an allogeneic mixed leukocyte reaction (Figure 5; *see* Figure E2). $CD11c^+$, $CD14^+$, and $CD1c^+$ cells were enriched from single-cell lung suspensions using positive selection and then assessed by flow cytometric analysis. Cytospins of isolated cells showed distinct morphologies of enriched cell populations. All $CD11c^+$ cells enriched from lung digest and alveolar macrophages isolated from BAL fluid efficiently stimulated naïve $CD4^+$ and $CD8^+$ T-cell proliferation (Figure 5). However, the $CD1c^+$ MPs (including both $CD1a^{+/-}$ ModCs and pulmonary DCs) were the most potent allo-stimulators, inducing more CD4 and CD8 T-cell proliferation than $CD14^+$ MPs (including tissue monos and both $CD1a^{+/-}$ ModCs) and alveolar macrophages (Figure 5). Thus, the mixed leukocyte reaction suggests that $CD1c^+$ MPs are superior T-cell stimulators.

Preliminary Transcriptome Analysis of Human Lung and Blood MPs

To determine expression for genes selectively associated with DCs, monocytes and/or macrophages, we analyzed mRNA from sorted pulmonary and blood MPs from three to four donors (donors, *see* Table E1) (32–35). Preliminary transcriptome analysis illustrated that *Clec9a* was selectively expressed by blood $CD141^+$ DCs, and not by any lung DCs, monocytes-derived cells, or macrophages (Figure 6). In contrast, Langerin (*CD207*), *CCR7, CD86, CD80,* and *CD40* mRNA transcript expression was greatest in pulmonary DCs and $CD1a^+$ ModCs compared with blood DCs (Figure 6). Similar to protein expression, thrombomodulin (*CD141*) was expressed by most lung MPs and $CD141^+$ blood DCs, whereas there was little to no expression observed for pulmonary DCs, blood monocytes, and blood $CD1c^+$ DCs. Pulmonary DCs, $CD1a^+$ ModCs, and blood $CD141^+$ DCs expressed the highest levels

Table 2. A Summary of Endocytic Receptors, Chemokine Receptors, and Integrins Expressed by $CD11c^+$ HLA-$DR^{int}CD141^+CD14^+$ and HLA-$DR^{hi}CD1c^+DEC205^+$ Mononuclear Phagocytes Found in Lung Lymph Nodes

	$CD14^+CD141^+$ MP	$CD1c^+$ MP
CD11c	++	++
HLA-DR	+	+++
CD206	+	−
CD14	+	−
CD16	+	−
CD11b	+	−
CD141	+	−
CD1c	−	int/+
CD1a	−/lo	lo/+
DEC205	−	+
Clec9a	−	−
CD64	+	−
CD36	+	−
CCR2	+	−
CCR7	−	+

Definition of abbreviations: HLA = human leukocyte antigen; int = intermediate; lo = low; MP = mononuclear phagocyte.

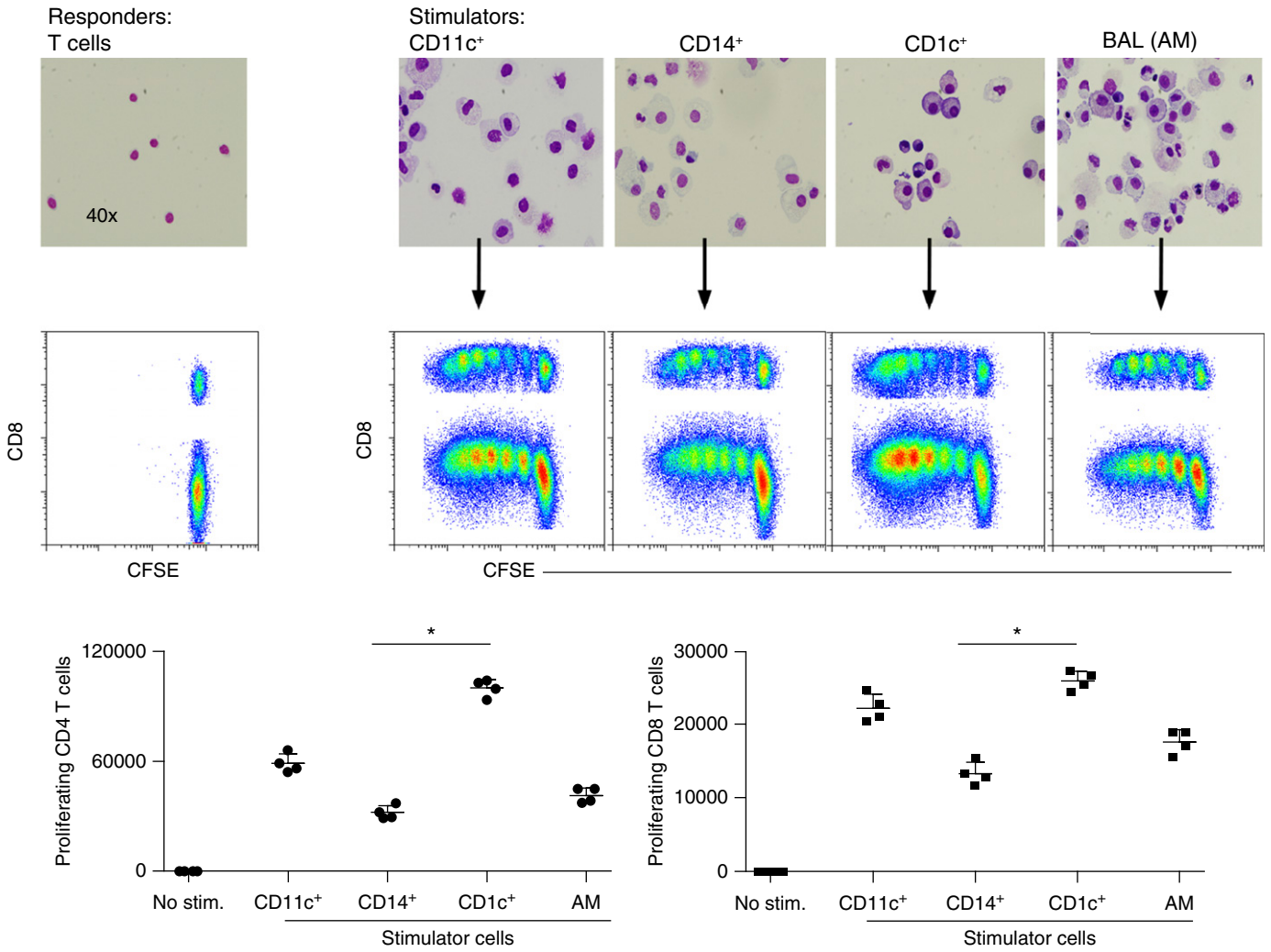

Figure 5. Assessment of the immune-stimulatory capacity of $CD11c^+$ human leukocyte antigen–DR^+ mononuclear phagocytes (MPs) isolated from human lung. Carboxyfluorescein succinimidyl ester (CFSE)-labeled $CD3^+$ T cells isolated from peripheral blood mononuclear cells were stimulated for 5 days with enriched allogeneic lung MP populations; $CD11c^+$, $CD14^+$, and $CD1c^+$ cells obtained from tissue and alveolar macrophages (AM) obtained from bronchoaveolar lavage (BAL). Cytospins of each enriched cell population were stained using Diff-Quick (*upper panel*). Proliferation of responding T cells was assessed by fluorescence-activated cell sorter and measured by CFSE dilution. Total cell counts of proliferating $CD4^+$ T cells and $CD8^+$ T cells from each co-culture, in quadruplets, were plotted. $^*P < 0.001$. Data comparing the mixed leukocyte reaction for $CD14^+$ and $CD1c^+$ MPs is one representative experiment of three independent experiments. Stim = stimulator cells.

of *ID2* and *Flt3,* which have been shown to be necessary for DC development. Pulmonary DCs and $CD1a^+$ ModCs uniquely express RUNX3, a transcription factor that regulates pulmonary DC responsiveness to tumor growth factor-β (36). All $CD1c^+$ MPs in the lung expressed the transcription factor Zbtb46, which is a transcription factor expressed by murine tissue DCs and an inflammatory monocytes subset (37, 38). Specifically, pulmonary DCs displayed the greatest expression of Zbtb46 compared with other cell populations analyzed from both the lungs and blood. As expected, human alveolar macrophages had the highest levels of known phagocytic genes and pattern recognition receptors: *MARCO*, *PPARγ*, *CCL18*, *GCHFR, CAMP, LAMP1, TLR4,* and *CD71.* In summary, preliminary transcriptome analysis suggests MP populations of the lung and blood have distinct gene expression profiles.

Lung Vascular Perfusion Reduces the Frequency of Blood DCs

Lastly, we analyzed MP populations found in resected lung tissue from subjects with non-small cell lung carcinoma that were unable to be perfused. In tumor-bearing tissues, we observed enhanced frequencies of $Clec9a^+$ DCs and $CD303^+$ pDCs that were detected in blood, but which were not detected in tumor-free tissues (Figure 7A; *see* Figure E1) (39). In line with previous studies, elevated numbers of $CD303^+$ pDCs were detected in cell suspensions of non-small cell carcinoma, peritumoral lung tissue, and pulmonary LNs obtained from the same donor. However, no pDCs were observed in tumor-free lung tissue and its associated LNs (Figure 7A and 7B; *see* Figure E4) (40). The observed differences in MP populations found in resected tumor-bearing lung tissues could either be due to contaminating blood MPs within the

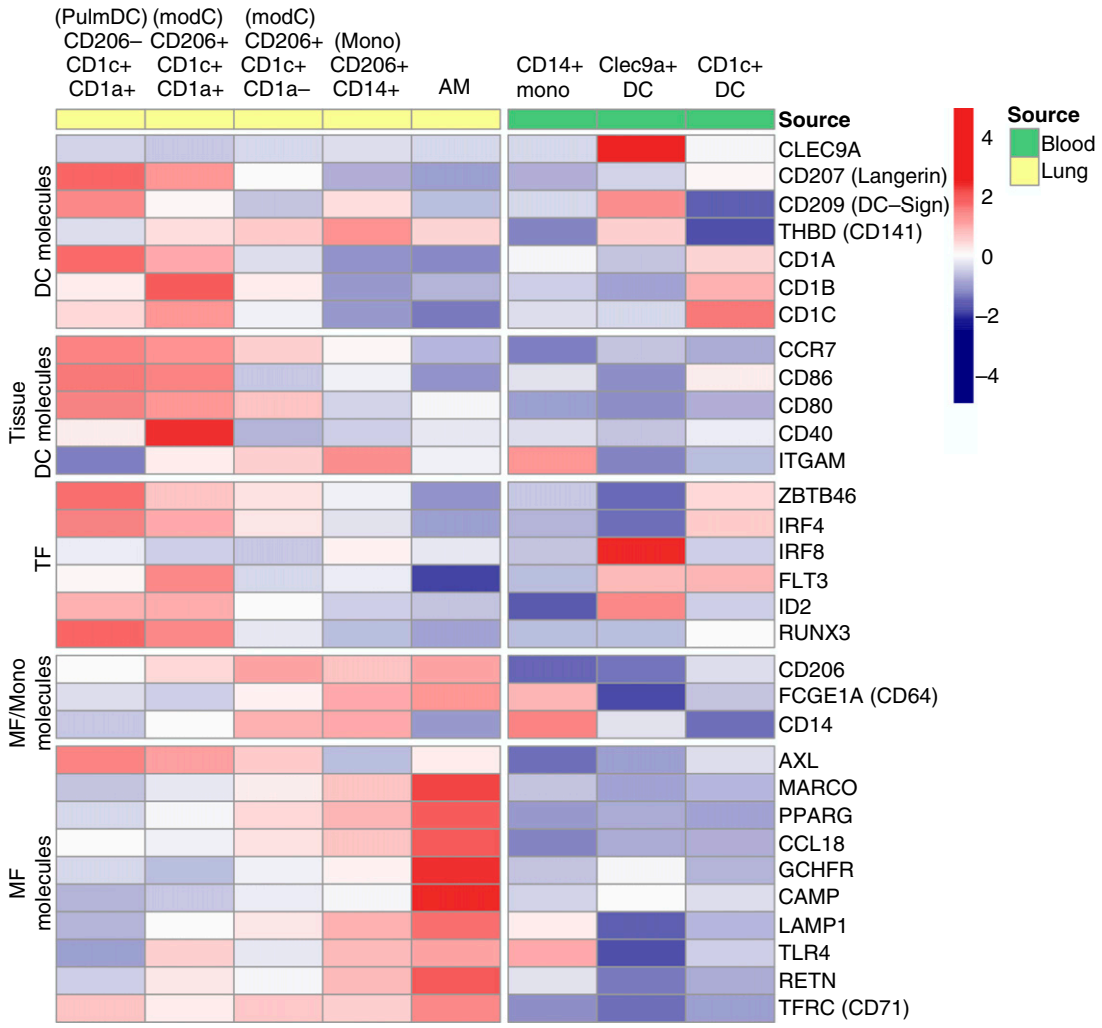

Figure 6. Preliminary transcriptome analysis of sorted human lung and peripheral blood mononuclear phagocytes. Heatmap shows average expression in each cell type for dendritic cell (DC) molecules, tissue DC molecules, transcription factors (TF), shared macrophage (MF) and monocyte (Mono) molecules, and macrophage molecules. Averages were calculated using a matrix that normalized using variance-stabilizing normalization. Row scale (*red–blue*) demonstrates expression level after subtracting the average expression and dividing by the SD of that row. Data represents gene expression from at least three to four individual donors per cell type. AM = alveolar macrophage; ModC = monocyte-derived cell.

vasculature that were not removed by perfusion or recruited blood-like MPs that infiltrated the tissue.

The pulmonary arteries of all tumor-free lungs were flushed with cold storage solution at the time of organ procurement. However, the extent of perfusion was variable, and therefore, upon arrival in the laboratory, lungs were perfused a second time to enhance the removal of blood contaminants. After a second perfusion, digested lung tissue contained fewer blood DCs ($CD11b^-$ $CD14^-$, green gate), including both $CD1c^+$ and $CD141^+$ DCs, compared with lungs only perfused during the procurement (Figure 7C). $CD14^+$ MPs in twice-perfused lungs uniformly co-expressed CD141 with a spectrum of CD1c expression, which was not observed with blood $CD14^+$ monocytes (Figure 7). Thus, compared with resected tumor-bearing lungs or lungs perfused only once during procurement, acquired nondiseased lungs with intact vasculature allowed for the removal of excess blood MPs via additional perfusions.

Discussion

In the past decade, the identification of distinct MP subpopulations with unique functions and origins in mice has provided the impetus to find human correlates. Using multiparameter cytometry and gene-expression profiling, the identification of MP populations in human tissues has become possible (26, 41). However, the ability to identify tissue resident MPs has been limited by the health and availability of human tissues. Our goal was to characterize tissue-resident MPs in nondiseased lungs, which was contingent on the ability to distinguish extravascular tissue MPs from MPs in the vascular lumen. In this study, five extravascular MPs were identified and defined based on phenotype, location, and gene expression. In addition to alveolar macrophages, four cell types demonstrated the ability to access the airspace-delivered antibody and

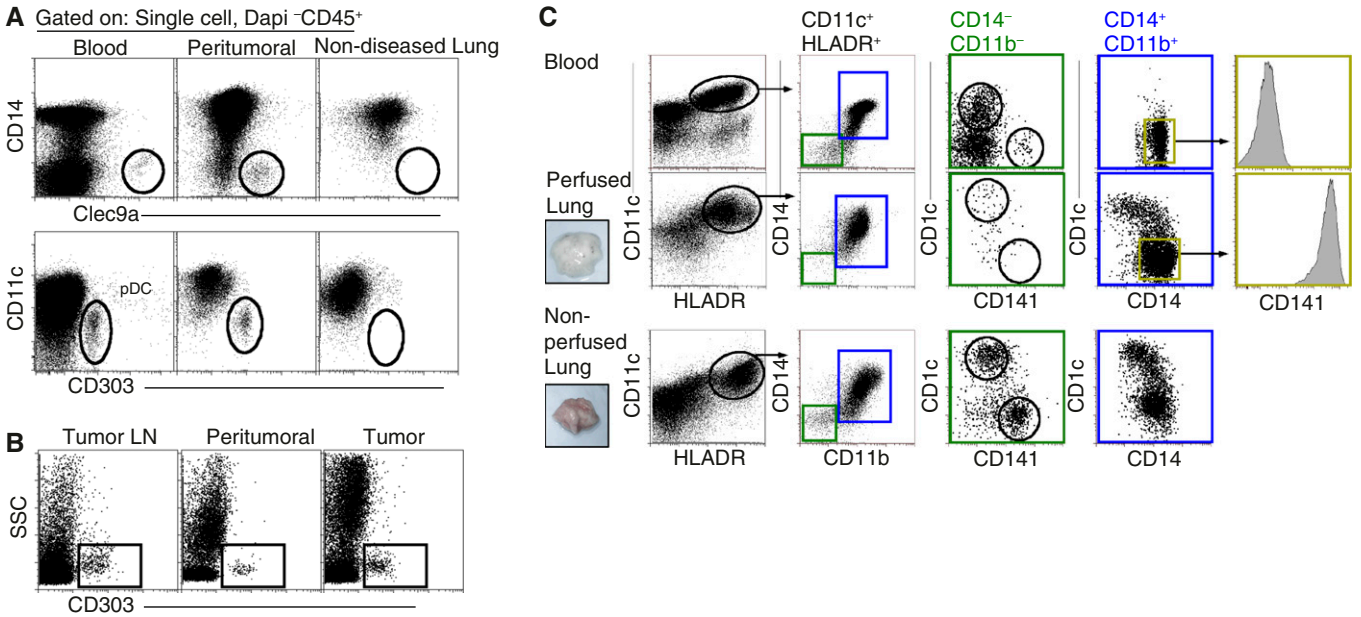

Figure 7. Phenotypic analyses of mononuclear phagocytes (MPs) isolated from perfused and nonperfused lung tissue, tumor-bearing tissues, and peripheral blood. (*A*) Flow cytometric analysis of Clec9a$^+$ dendritic cells (DCs) and plasmacytoid DCs (pDCs) (CD303$^+$) in blood, nonperfused peritumoral lung tissue and perfused tumor-free lung tissue. Data shown are representative of at least eight independent experiments. (*B*) Analysis of CD303$^+$ pDCs found in tissues obtained from a patient with non–small cell lung carcinoma: hilar lymph node (LN), tumor-adjacent tissue, and adenocarcinoma. Data are one representative experiment of at least two independent experiments. (*C*) Flow cytometric analysis of MPs obtained from peripheral blood (*upper panel*) and enzymatically dispersed lung tissue that was twice perfused (*middle panel*) or nonperfused (*lower panel*). Representative tissues shown (*insets*). Gated CD11c$^+$HLA-DR$^+$ MPs were first plotted as CD14 versus CD11b. CD14$^-$CD11b fractions (*green gate*) were detected in the blood and nonperfused lung and plotted as CD1c versus CD141 to reveal blood DC populations. CD14$^+$CD11b$^+$ cells (*blue gate*) were plotted as CD1c versus CD141 to demonstrate phenotypic differences between MPs of the lung and blood. CD1c$^-$CD14$^+$CD11b$^+$ MPs (*yellow gate*) representing blood monocytes and tissue monocytes were assessed for CD141 expression. Data are representative of at least 15 independent experiments from different donors. DAPI = 4′,6-diamidino-2-phenylindole; HLA = human leukocyte antigen; SSC = side scatter.

stimulate T cells in a mixed-leukocyte reaction. Our findings support the growing recognition of myeloid cell diversity in tissues. However, the identified monocytes, monocyte-derived cells, and DCs in nondiseased human lungs differed from other MPs, particularly DCs, which have been previously described in human blood, lymphoid tissues, and other mucosal sites.

Because most acquired human lung tissue will not feasibly allow the identification of MPs present within the extravascular routes versus intravascular routes, we set out to find a marker that could distinguish these two compartments. Analyses of more than 72 nondiseased human lungs consistently revealed that CD206 is exclusively expressed on alveolar macrophages and three subsets of CD14$^+$ MPs (CD14$^+$ tissue monocytes and CD1a$^{+/-}$ ModCs). Importantly, CD206 expression was not detected on cells found in blood or in the intravascular compartment of the lung. The mannose receptor, CD206, recognizes a wide range of micro-organisms, facilitates the uptake of mannose-coated particles and mannosylated proteins, and can assist in antigen presentation (42, 43). The mannose receptor has also been implicated in the clearance of apoptotic cells in patients with COPD, where alveolar macrophages express less CD206 compared with alveolar macrophages from healthy control subjects (44). Therefore, CD206 expression by pulmonary MPs is requisite for the recognition and clearance of invading microbes and for the maintenance of tissue homeostasis. Interestingly, blood monocytes cultured with IL-4 and granulocyte-macrophage colony-stimulating factor can up-regulate both CD206 and CD1a (45). Therefore, although CD206 distinguishes tissue MPs from blood MPs, it does not exclude the possibility that tissue MPs derive from monocyte precursors in the blood. Intriguingly, one extravascular MP, pulmonary DCs, did not express the mannose receptor. In the skin, CD206 expressing CD1a$^+$ DCs have been shown to down-regulate CD206 during maturation, which may coincide with diminished endocytosis that occurs during DC maturation (45, 46). CD1a$^+$ ModCs and pulmonary DCs share many overlapping surface markers and gene expression. Therefore, it is possible that pulmonary DCs represent maturing LN-bound CD1a$^+$ ModCs that lose CD206 expression or a pulmonary MP that never up-regulated CD206 at all.

Extravascular and intravascular CD14$^+$ MPs share similar size, morphology, and surface molecule expression for CD14, CD11b, CCR2, and CD16. However, in addition to CD206, extravascular CD14$^+$ MPs displayed higher levels of expression for CD141, CD11c, HLA-DR, and CCR7 compared with the intravascular CD14$^+$ monocytes. These data suggest that extravascular CD14$^+$ MPs may derive from intravascular CD14$^+$ monocytes. Evidence from mouse studies has demonstrated that blood-derived monocytes up-regulate CD11c, MHCII, CCR7, and CD206 upon entering tissues while maintaining multiple properties of intravascular monocytes, including size and the expression of CD64

(1, 6, 8, 47). Similar $CD141^+CD14^+$ MPs were found in lung and lung-draining LNs with similar phenotypes and expression of chemokine receptor CCR2. Within lung-draining LNs, $CD141^+CD14^+$ pulmonary MPs localized to T-cell zones, suggesting that these monocyte-derived MPs may play a role in regulating adaptive immunity. After human skin engraftment in immune-deficient mice, dermal $CD141^+CD14^+$ MPs migrated to the skin-draining LNs (48); thus, if these dermal MPs are the equivalent of the lung MPs, this study would suggest that pulmonary $CD141^+CD14^+$ MPs might also have a migratory capacity.

DCs are the most potent antigen-presenting cells that exist in both the lung and lung-draining LNs (49, 50). We detected a similar $CD14^+CD141^+$ ModC and pulmonary DC populations in both the lungs and associated LNs. Our cumulative data suggest $CD1c^+$ LN cells are pulmonary DCs based on morphology (time-lapsed video), transcriptome analysis, high protein expression of HLA-DR and CCR7, and gene expression of Zbtb46 and Langerin. Moreover, a Langerin-expressing $CD206^-CD14^{lo}CD1c^+CD1a^+$ MP population was found in the lungs of subjects with COPD, indicating a similar cell population was previously reported (51). Due to immune-stimulatory capacity in mixed leukocyte reactions and localization to the T-cell zone of LNs, the pulmonary DCs defined in this study most likely play a prominent role in linking innate and adaptive immunity. Lastly, we did not observe the presence of blood equivalent DCs in nondiseased lung-draining LNs ($CD14^-CD141^+Clec9a^+$ blood DCs or pDCs).

Overall, in an effort to conduct a comprehensive phenotypic study, we were prudent in our selection of lungs from subjects with minimal inflammation and smoking history. In this study, we used flow cytometry to identify extravascular pulmonary MPs distinct from intravascular and blood MPs. Pulmonary MPs can be defined minimally by using forward scatter, SSC, CD45, HLA-DR, CD206, CD14, CD1c, and CD1a, along with stains to exclude lymphocyte lineage and dead or nonviable cells, which is absolutely essential. Alveolar macrophages can be detected by their distinctive high SSC, which was a log-fold greater than neutrophils and other MPs in the lung, low CD14-expression, and high expression for CD206 and CD64. It can be concluded that five distinct MP populations exist in a disease-free lung: four CD206 expressing MPs, including alveolar macrophages, tissue monocytes, and $CD1a^+$ and $CD1a^-$ ModCs; and one pulmonary $CD1c^+CD1a^+$ DC that does not express the mannose receptor. Importantly, among the 72 donor lungs included in this study, the MP populations defined in the lung and lung-draining LNs were consistently observed across the subjects' age, sex, and genetic background. The present study was performed using relatively healthy donor lungs and establishes a resource for future functional studies in disease states. ■

Author disclosures are available with the text of this article at www.atsjournals.org.

Acknowledgment: The authors thank Dr. Sonia M. Leach in the Department of Integrated Center for Genes at National Jewish Health for her assistance in biostatistical analysis. This study is dedicated to the lung donors and their families who enabled this research.

References

1. Guilliams M, Lambrecht BN, Hammad H. Division of labor between lung dendritic cells and macrophages in the defense against pulmonary infections. *Mucosal Immunol* 2013;6:464–473.
2. Guilliams M, Ginhoux F, Jakubzick C, Naik SH, Onai N, Schraml BU, Segura E, Tussiwand R, Yona S. Dendritic cells, monocytes and macrophages: a unified nomenclature based on ontogeny. *Nat Rev Immunol* 2014;14:571–578.
3. Schulz C, Gomez Perdiguero E, Chorro L, Szabo-Rogers H, Cagnard N, Kierdorf K, Prinz M, Wu B, Jacobsen SE, Pollard JW, *et al*. A lineage of myeloid cells independent of Myb and hematopoietic stem cells. *Science* 2012;336:86–90.
4. Hashimoto D, Chow A, Noizat C, Teo P, Beasley MB, Leboeuf M, Becker CD, See P, Price J, Lucas D, *et al*. Tissue-resident macrophages self-maintain locally throughout adult life with minimal contribution from circulating monocytes. *Immunity* 2013;38:792–804.
5. Gomez Perdiguero E, Klapproth K, Schulz C, Busch K, Azzoni E, Crozet L, Garner H, Trouillet C, de Bruijn MF, Geissmann F, *et al*. Tissue-resident macrophages originate from yolk-sac-derived erythro-myeloid progenitors. *Nature* 2015;518:547–551.
6. Jakubzick C, Gautier EL, Gibbings SL, Sojka DK, Schlitzer A, Johnson TE, Ivanov S, Duan Q, Bala S, Condon T, *et al*. Minimal differentiation of classical monocytes as they survey steady-state tissues and transport antigen to lymph nodes. *Immunity* 2013;39: 599–610.
7. Tamoutounour S, Guilliams M, Montanana Sanchis F, Liu H, Terhorst D, Malosse C, Pollet E, Ardouin L, Luche H, Sanchez C, *et al*. Origins and functional specialization of macrophages and of conventional and monocyte-derived dendritic cells in mouse skin. *Immunity* 2013;39: 925–938.
8. Plantinga M, Guilliams M, Vanheerswynghels M, Deswarte K, Branco-Madeira F, Toussaint W, Vanhoutte L, Neyt K, Killeen N, Malissen B, *et al*. Conventional and monocyte-derived CD11b(+) dendritic cells initiate and maintain T helper 2 cell-mediated immunity to house dust mite allergen. *Immunity* 2013;38:322–335.
9. Janssen WJ, Barthel L, Muldrow A, Oberley-Deegan RE, Kearns MT, Jakubzick C, Henson PM. Fas determines differential fates of resident and recruited macrophages during resolution of acute lung injury. *Am J Respir Crit Care Med* 2011;184: 547–560.
10. Rivollier A, He J, Kole A, Valatas V, Kelsall BL. Inflammation switches the differentiation program of Ly6Chi monocytes from antiinflammatory macrophages to inflammatory dendritic cells in the colon. *J Exp Med* 2012;209:139–155.
11. Demedts IK, Bracke KR, Maes T, Joos GF, Brusselle GG. Different roles for human lung dendritic cell subsets in pulmonary immune defense mechanisms. *Am J Respir Cell Mol Biol* 2006;35: 387–393.
12. Demedts IK, Brusselle GG, Vermaelen KY, Pauwels RA. Identification and characterization of human pulmonary dendritic cells. *Am J Respir Cell Mol Biol* 2005;32:177–184.
13. Masten BJ, Olson GK, Tarleton CA, Rund C, Schuyler M, Mehran R, Archibeque T, Lipscomb MF. Characterization of myeloid and plasmacytoid dendritic cells in human lung. *J Immunol* 2006;177: 7784–7793.
14. Tsoumakidou M, Kemp SJ, Thorley AJ, Zhu J, Dewar A, Jeffery PK, Tetley TD. Expression of blood dendritic cell antigens (BDCAs) by CD1a+ human pulmonary cells. *Respir Med* 2009;103: 935–938.
15. Haniffa M, Shin A, Bigley V, McGovern N, Teo P, See P, Wasan PS, Wang XN, Malinarich F, Malleret B, *et al*. Human tissues contain CD141hi cross-presenting dendritic cells with functional homology to mouse CD103+ nonlymphoid dendritic cells. *Immunity* 2012;37: 60–73.
16. Schlitzer A, McGovern N, Teo P, Zelante T, Atarashi K, Low D, Ho AW, See P, Shin A, Wasan PS, *et al*. IRF4 transcription factor-dependent CD11b+ dendritic cells in human and mouse control mucosal IL-17 cytokine responses. *Immunity* 2013;38:970–983.

17. Yu CI, Becker C, Wang Y, Marches F, Helft J, Leboeuf M, Anguiano E, Pourpe S, Goller K, Pascual V, *et al*. Human CD1c+ dendritic cells drive the differentiation of CD103+ CD8+ mucosal effector T cells via the cytokine TGF-β. *Immunity* 2013;38:818–830.
18. Downey GP, Doherty DE, Schwab B III, Elson EL, Henson PM, Worthen GS. Retention of leukocytes in capillaries: role of cell size and deformability. *J Appl Physiol (1985)* 1990;69:1767–1778.
19. Doerschuk CM, Downey GP, Doherty DE, English D, Gie RP, Ohgami M, Worthen GS, Henson PM, Hogg JC. Leukocyte and platelet margination within microvasculature of rabbit lungs. *J Appl Physiol (1985)* 1990;68:1956–1961.
20. Doerschuk CM, Allard MF, Martin BA, MacKenzie A, Autor AP, Hogg JC. Marginated pool of neutrophils in rabbit lungs. *J Appl Physiol (1985)* 1987;63:1806–1815.
21. Anderson KG, Mayer-Barber K, Sung H, Beura L, James BR, Taylor JJ, Qunaj L, Griffith TS, Vezys V, Barber DL, *et al*. Intravascular staining for discrimination of vascular and tissue leukocytes. *Nat Protoc* 2014;9:209–222.
22. Rich EN, Desch AN, Henson PM, Jakubzick C. Characterizing the human orthologues of murine pulmonary dendritic cell populations [abstract]. *Am J Respir Crit Care Med* 2011;183:A2837.
23. Li H, Durbin R. Fast and accurate short read alignment with Burrows-Wheeler transform. *Bioinformatics* 2009;25:1754–1760.
24. Huber W, von Heydebreck A, Sültmann H, Poustka A, Vingron M. Variance stabilization applied to microarray data calibration and to the quantification of differential expression. *Bioinformatics* 2002;18: S96–S104.
25. Robinson MD, McCarthy DJ, Smyth GK. edgeR: a Bioconductor package for differential expression analysis of digital gene expression data. *Bioinformatics* 2010;26:139–140.
26. Yu YR, Hotten DF, Malakhau Y, Volker E, Ghio AJ, Noble PW, Kraft M, Hollingsworth JW, Gunn MD, Tighe RM. Flow cytometric analysis of myeloid cells in human blood, bronchoalveolar lavage, and lung tissues. *Am J Respir Cell Mol Biol* 2016;54:13–24.
27. Kress H, Stelzer EH, Holzer D, Buss F, Griffiths G, Rohrbach A. Filopodia act as phagocytic tentacles and pull with discrete steps and a load-dependent velocity. *Proc Natl Acad Sci USA* 2007;104: 11633–11638.
28. Steinman RM, Cohn ZA. Identification of a novel cell type in peripheral lymphoid organs of mice. I. Morphology, quantitation, tissue distribution. *J Exp Med* 1973;137:1142–1162.
29. Förster R, Schubel A, Breitfeld D, Kremmer E, Renner-Müller I, Wolf E, Lipp M. CCR7 coordinates the primary immune response by establishing functional microenvironments in secondary lymphoid organs. *Cell* 1999;99:23–33.
30. del Rio ML, Rodriguez-Barbosa JI, Kremmer E, Förster R. CD103- and CD103+ bronchial lymph node dendritic cells are specialized in presenting and cross-presenting innocuous antigen to CD4+ and CD8+ T cells. *J Immunol* 2007;178:6861–6866.
31. Jakubzick C, Tacke F, Llodra J, van Rooijen N, Randolph GJ. Modulation of dendritic cell trafficking to and from the airways. *J Immunol* 2006;176:3578–3584.
32. Haldar M, Murphy KM. Origin, development, and homeostasis of tissue-resident macrophages. *Immunol Rev* 2014;262:25–35.
33. Epelman S, Lavine KJ, Randolph GJ. Origin and functions of tissue macrophages. *Immunity* 2014;41:21–35.
34. Murphy KM. Transcriptional control of dendritic cell development. *Adv Immunol* 2013;120:239–267.
35. Gautier EL, Shay T, Miller J, Greter M, Jakubzick C, Ivanov S, Helft J, Chow A, Elpek KG, Gordonov S, *et al*.; Immunological Genome Consortium. Gene-expression profiles and transcriptional regulatory pathways that underlie the identity and diversity of mouse tissue macrophages. *Nat Immunol* 2012;13:1118–1128.
36. Fainaru O, Woolf E, Lotem J, Yarmus M, Brenner O, Goldenberg D, Negreanu V, Bernstein Y, Levanon D, Jung S, *et al*. Runx3 regulates mouse TGF-beta-mediated dendritic cell function and its absence results in airway inflammation. *EMBO J* 2004;23:969–979.
37. Satpathy AT, Kc W, Albring JC, Edelson BT, Kretzer NM, Bhattacharya D, Murphy TL, Murphy KM. Zbtb46 expression distinguishes classical dendritic cells and their committed progenitors from other immune lineages. *J Exp Med* 2012;209:1135–1152.
38. Meredith MM, Liu K, Darrasse-Jeze G, Kamphorst AO, Schreiber HA, Guermonprez P, Idoyaga J, Cheong C, Yao KH, Niec RE, *et al*. Expression of the zinc finger transcription factor zDC (Zbtb46, Btbd4) defines the classical dendritic cell lineage. *J Exp Med* 2012;209: 1153–1165.
39. Segura E, Valladeau-Guilemond J, Donnadieu MH, Sastre-Garau X, Soumelis V, Amigorena S. Characterization of resident and migratory dendritic cells in human lymph nodes. *J Exp Med* 2012;209:653–660.
40. Vermi W, Soncini M, Melocchi L, Sozzani S, Facchetti F. Plasmacytoid dendritic cells and cancer. *J Leukoc Biol* 2011;90:681–690.
41. Bharat A, Bhorade SM, Morales-Nebreda L, Mc Quattie-Pimentel AC, Soberanes S, Ridge K, DeCamp MM, Mestan KK, Perlman H, Budinger GR, *et al*. Flow cytometry reveals similarities between lung macrophages in humans and mice. *Am J Respir Cell Mol Biol* 2016:54:147–149.
42. Kerrigan AM, Brown GD. C-type lectins and phagocytosis. *Immunobiology* 2009;214:562–575.
43. Sallusto F, Cella M, Danieli C, Lanzavecchia A. Dendritic cells use macropinocytosis and the mannose receptor to concentrate macromolecules in the major histocompatibility complex class II compartment: downregulation by cytokines and bacterial products. *J Exp Med* 1995;182:389–400.
44. Hodge S, Hodge G, Scicchitano R, Reynolds PN, Holmes M. Alveolar macrophages from subjects with chronic obstructive pulmonary disease are deficient in their ability to phagocytose apoptotic airway epithelial cells. *Immunol Cell Biol* 2003;81:289–296.
45. Wollenberg A, Mommaas M, Oppel T, Schottdorf EM, Günther S, Moderer M. Expression and function of the mannose receptor CD206 on epidermal dendritic cells in inflammatory skin diseases. *J Invest Dermatol* 2002;118:327–334.
46. Garrett WS, Chen LM, Kroschewski R, Ebersold M, Turley S, Trombetta S, Galán JE, Mellman I. Developmental control of endocytosis in dendritic cells by Cdc42. *Cell* 2000;102:325–334.
47. Crane MJ, Daley JM, van Houtte O, Brancato SK, Henry WL Jr, Albina JE. The monocyte to macrophage transition in the murine sterile wound. *PLoS One* 2014;9:e86660.
48. Chu CC, Ali N, Karagiannis P, Di Meglio P, Skowera A, Napolitano L, Barinaga G, Grys K, Sharif-Paghaleh E, Karagiannis SN, *et al*. Resident CD141 (BDCA3)+ dendritic cells in human skin produce IL-10 and induce regulatory T cells that suppress skin inflammation. *J Exp Med* 2012;209:935–945.
49. Desch AN, Randolph GJ, Murphy K, Gautier EL, Kedl RM, Lahoud MH, Caminschi I, Shortman K, Henson PM, Jakubzick CV. CD103+ pulmonary dendritic cells preferentially acquire and present apoptotic cell-associated antigen. *J Exp Med* 2011;208:1789–1797.
50. Lambrecht BN, Hammad H. Lung dendritic cells in respiratory viral infection and asthma: from protection to immunopathology. *Annu Rev Immunol* 2012;30:243–270.
51. Van Pottelberge GR, Bracke KR, Demedts IK, De Rijck K, Reinartz SM, van Drunen CM, Verleden GM, Vermassen FE, Joos GF, Brusselle GG. Selective accumulation of langerhans-type dendritic cells in small airways of patients with COPD. *Respir Res* 2010;11:35.